

## Microscopic Origin of the Hofmeister Effect in Gelation Kinetics of Colloidal Silica

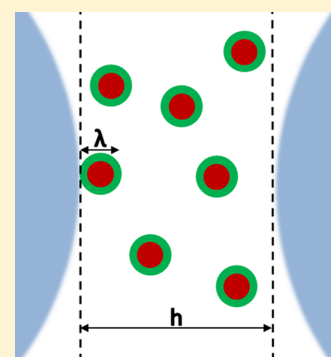
Marte van der Linden,<sup>†,||</sup> Breannán O. Conchúir,<sup>†,||</sup> Elisabetta Spigone,<sup>†</sup> Arun Niranjana,<sup>†</sup> Alessio Zaccone,<sup>\*,†,‡</sup> and Pietro Cicuti<sup>\*,†</sup>

<sup>†</sup>Cavendish Laboratory, University of Cambridge, Madingley Road, Cambridge CB3 0HE, United Kingdom

<sup>‡</sup>Physics Department and Institute for Advanced Study, Technische Universität München, Lichtenbergstrasse 2 a, Garching 85748, Germany

### Supporting Information

**ABSTRACT:** The gelation kinetics of silica nanoparticles is a central process in physical chemistry, yet it is not fully understood. Gelation times are measured to increase by over 4 orders of magnitude, simply changing the monovalent salt species from CsCl to LiCl. This striking effect has no microscopic explanation within current paradigms. The trend is consistent with the Hofmeister series, pointing to short-ranged solvation effects not included in the standard colloidal (DLVO) interaction potential. By implementing a simple form for short-range repulsion within a model that relates the gelation timescale to the colloidal interaction forces, we are able to explain the many orders of magnitude difference in the gelation times at fixed salt concentration. The model allows us to estimate the magnitude of the non-DLVO hydration forces, which dominate the interparticle interactions on the length scale of the hydrated ion diameter. This opens the possibility of finely tuning the gelation time scale of nanoparticles by just adjusting the background electrolyte species.



The total interaction potential in aqueous suspensions of charged colloidal particles is often taken as the sum of the van der Waals attraction and a simple approximation of the electrostatic double-layer repulsion, forming the classical Derjaguin–Landau–Verwey–Overbeek (DLVO) potential.<sup>1</sup> The electrostatic repulsion can be overcome by adding salt, thus increasing the screening of electrostatic repulsion, and lowering the energy barrier against aggregation.<sup>2</sup> Colloid particles then typically aggregate into clusters, which grow over time with the possibility of forming a sample-spanning network. Silica particles, and specifically Ludox, have been a classical model system for colloidal physical chemistry and also have a key place in industrial processing, coatings, ink receptive papers, metal casting, refractory products, and catalysts.

DLVO theory predicts that there is a salt concentration at which the suspension aggregates (critical coagulation concentration); here the maximum DLVO interaction and its derivative are both zero (i.e., there is no energy barrier against aggregation). This concentration is proportional to  $z^{-6}$ , where  $z$  is the valency of the salt ions and is one of the successes of DLVO theory.<sup>2,3</sup> It is well known that DLVO theory breaks down completely for high salt concentrations (above 0.1 M, which unfortunately is the regime of biological interest).<sup>4,5</sup> In this range, the basic assumptions of point charges, a solvent continuum and neglecting ion-surface adsorption and dispersion forces, are called into question. On a fundamental level, even the assumption that electrostatic forces and dispersion forces are additive is incorrect.<sup>6,7</sup>

It is shown in this Letter that there is a spectacular failure of DLVO theory in estimating gelation times, for identical

particles, in the presence of different monovalent salts even at low concentration. Changing the salt type dramatically affects the aggregation process. Using a model for relating the gelation kinetics to particle interactions, a non-DLVO hydration repulsion is characterized, and the dramatic changes in gelation kinetics are explained microscopically in terms of ion solvation and its interplay with the charged colloid surface. The proposed framework will make it possible to finely tune the gelation rate of nanoparticles simply by the choice of monovalent electrolyte species in the colloidal solution.

A minimum of context and concepts proposed to explain the Hofmeister series are useful to the reader. It was first shown by Hofmeister<sup>8</sup> that the stability of a colloidal solution (he made observations on proteins, which were then investigated by others,<sup>9</sup> while other work investigated colloidal particles<sup>7,10–12</sup>) can be drastically different upon the addition of different salts of the same valency, even if all other parameters (such as the salt concentration) are kept constant. Electrolytes could be arranged according to their efficiency in salting-out protein (now known as “Hofmeister series”). The effect is understood to be related to how salt ions structure the water around themselves. For monovalent cations the series is  $\text{NH}_4^+$ ,  $\text{Cs}^+$ ,  $\text{Rb}^+$ ,  $\text{K}^+$ ,  $\text{Na}^+$ ,  $\text{Li}^+$ , from most chaotropic (weakly hydrated, structure breakers) to most kosmotropic (strongly hydrated, structure makers), and which extreme is most destabilizing depends on the surface properties of the colloids.<sup>13</sup>

**Received:** June 18, 2015

**Accepted:** July 7, 2015

There are numerous, partially conflicting, theories as to the origin of these short-ranged ion-specific colloidal interactions, linking to the ionic size.<sup>12,14,15</sup> Strongly polarizable ions are large and have more diffuse electron clouds. The energy penalty for being less well hydrated (for example, due to adsorption at an interface) is low for such ions because the charge can be easily redistributed.<sup>16</sup> The decreasing size trend in going from chaotropic to cosmotropic in the Hofmeister series is consistent with this picture;<sup>11</sup> however, the effective polarizability of the ions consists of contributions from both the ion itself and the solvent molecules in its hydration shell;<sup>16</sup> This by extension may significantly augment the dispersion forces and give further ion-specific interactions.<sup>17</sup> Another suggestion is that the large electric field on the colloidal surface, arising from the finite size of the counterions, results in the ions acquiring appreciably large effective polarizabilities.<sup>18</sup>

Experiments with (negatively charged) mica surfaces showed that there is adsorption of cations. More hydrated cations (such as  $\text{Li}^+$ ) are adsorbed only at high salt concentrations, while the less hydrated ions adsorb at lower concentrations; however, once adsorbed, the cosmotropic ions retain part of their hydration layer. This gives rise to a repulsive interaction as two surfaces approach each other.<sup>2</sup> For mica, for example, cosmotropic ions are thus much more efficient at providing stabilization than chaotropic ions.

Models have been made to describe ion-specific distribution of ions near surfaces and their surface adsorption: An important factor is the ion diameter and whether the ions are hydrated.<sup>11</sup> Chaotropic ions have smaller effective diameters (as they are not hydrated), and they can adsorb to the surface. On the basis of this model, it was possible to calculate the critical coagulation concentration for a range of salts.<sup>11</sup>

A fully quantitative description of hydration interactions should include all factors previously outlined (finite ion sizes, discrete nature of the solvent, many-body dispersion forces, and polarization effects). Such a description does not exist and is beyond the scope of this Letter, which instead aims to provide motivation, guidance, and useful constraints for future models. We take a simplified approach to modeling the hydration interactions, which is described later, and we show how the total interparticle interaction can be related to the gelation times and thus measured. The DVLO potential  $V_{\text{DVLO}}$  is a linear superposition of an attractive van der Waals potential  $V_{\text{vdW}}$ , an electrostatic repulsion potential  $V_{\text{R}}$ , and a short-ranged Born repulsion potential  $V_{\text{B}}$ , which we neglect in this study due to the fact it does not impact on the gelation process. The attractive component is given by

$$V_{\text{vdW}}(r) = \frac{-A_{\text{H}}(r)}{6} \left( \frac{2a^2}{r^2 - 4a^2} + \frac{2a^2}{r^2} + \log \frac{r^2 - 4a^2}{r^2} \right) \quad (1)$$

where  $a$  is the colloid radius and  $r = 2a + h$  is the colloidal center-to-center separation; see Figure 1a. The Hamaker function  $A_{\text{H}}$  can be written in the form<sup>20</sup>  $A_{\text{H}}(r) = A_{\epsilon=0} f_{\text{scr}}(r) + A_{\epsilon>0} f_{\text{ret}}(r)$ , where  $A_{\epsilon=0}$  is the zero frequency contribution that is screened by the counterions through the screening function  $f_{\text{scr}}(r)$  and  $A_{\epsilon>0}$  is the nonzero frequency contribution that is mitigated by retardation through the retardation function  $f_{\text{ret}}(r)$ . (Their full form is given in the SI for completeness.)

The DLVO theory is based on a number of assumptions, the most important of which is the linearized Poisson–Boltzmann treatment of the electric-double layer repulsion, which is valid

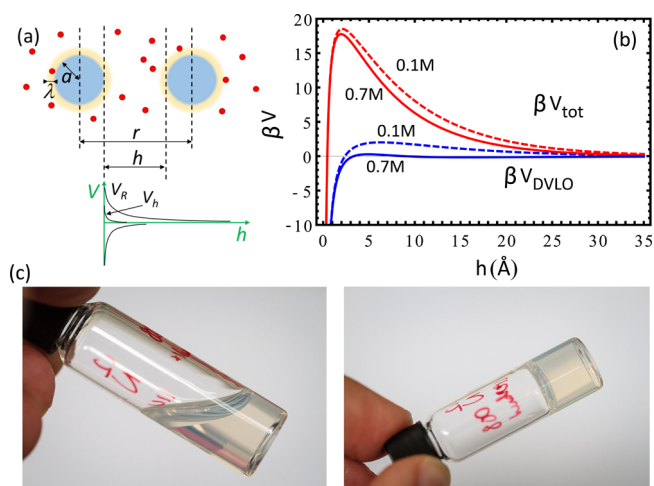


**Figure 1.** Time required for gelation of the sample is related to the interparticle interaction potential, and the specific hydration of the ions has a huge effect, controlling the intercolloid hydration repulsion at a  $h < \lambda$ . (a) Schematic and (b) plot of the “total” interaction obtained in this work, including the strongly ion-specific short-ranged repulsive hydration potential. Also illustrated are the classical terms in the DVLO interaction. At very short distances, on the order of the hydrated ionic diameter, the repulsive shoulder dominates the interaction. (c) Macroscopic sample initially flows as the vial is inverted (left), while after some time it becomes solid (right). This sample has  $\phi_{\text{Ludox}} = 0.140$  and 374 mM NaCl.

only within the Debye–Hückel limit for the surface potential, that is, for potentials lower than 20–25 mV. In our calculations, however, we used an extension due to Sader, Carnie, and Chan,<sup>21</sup> which extends the validity of DLVO theory to much higher potentials

$$V_{\text{R}} = 4\pi\epsilon_0\epsilon_m \left( \frac{k_{\text{B}}T}{e} \right)^2 Y(r)^2 \frac{a^2}{r} \ln[1 + \exp(-\kappa h)] \quad (2)$$

where  $\epsilon_0$  is the permittivity of free space,  $\epsilon_m$  is the relative permittivity of water,  $k_{\text{B}}$  is the Boltzmann constant,  $e$  is the counterion charge, and  $T$  is the temperature. The function  $Y(r)$  is given in full in the SI and depends on the surface potential  $\psi_0$ .

The other assumptions of the theory are the following: (a) The ions are treated as point-like. (Their finite volume and excluded-volume effects are neglected.) (b) Spatial correlations among ions are neglected; (c) Ion adsorption on the colloid surface is neglected. (d) Dissociation equilibria between charged species on the colloid surface and ions in solution are neglected. Many studies have shown that the interparticle potential deviates significantly from DLVO theory below a surface-to-surface separation  $h$  of  $\sim 2$  nm in water.<sup>22</sup> An additional repulsive potential has been postulated to arise from the hydration of the water due to the presence of counterions or on strongly hydrophilic surfaces. This potential is still not fully understood microscopically and, as previously outlined, there are different competing theories relating to its origins exist in the literature. Since the 1970s there has been a general agreement that the effective hydration potential decreases exponentially from the surface<sup>23</sup> and can thus be taken to have the following general form

$$V_{\text{h}} = F_0 \pi a \lambda^2 \exp\left(-\frac{h}{\lambda}\right) \quad (3)$$

where the fitting parameters  $F_0$  and  $\lambda$  control the magnitude and the decay of the potential, respectively. This expression has been used quantitatively to successfully describe the huge energy barrier contributed by repulsion between structured water layers on hydrophilic surfactant-coated colloids, a big effect that cannot be explained by DLVO theory alone.<sup>24</sup>

The full potential we consider is then a sum of dispersion, electrostatic, and surface hydration terms

$$V_{\text{tot}} = V_{\text{vdW}} + V_{\text{R}} + V_{\text{h}} \quad (4)$$

The interaction potential and gelation time are linked: A recent theoretical study<sup>25</sup> has established that the gelation time  $t_{\text{gel}}$  can be evaluated according to the following expression

$$t_{\text{gel}} = \frac{1}{2k_{\text{c}}[(1+c)\phi_0/2]^{d_{\text{f}}/3}} \quad (5)$$

where  $d_{\text{f}}$  is the fractal dimension of the clusters (which for reaction limited aggregation RLCA is  $d_{\text{f}} = 2.1$ <sup>26</sup>) and  $\phi_0 = (4/3)\pi a^3 n_0$  is the volume fraction of the colloids where  $n_0$  is the total number of colloidal particles per unit volume,  $n_0 = N/V$ . The parameter  $c$  equates to  $c = (1 - \phi_{\text{c}})/\phi_{\text{c}}$ , where  $\phi_{\text{c}}$  is the critical volume fraction at which the systems gels (the zero-shear viscosity diverges), which for spherical-like clusters is  $\phi_{\text{c}} \approx 0.64$ . The characteristic aggregation rate  $k_{\text{c}}$  is given by the relation

$$k_{\text{c}} = \frac{n_0 k_{\text{agg}}}{2} \quad (6)$$

where  $k_{\text{agg}}$  is the rate constant of aggregation. The stability ratio  $W$  is defined as<sup>27,28</sup>

$$W = \frac{k_{\text{s}}}{k_{\text{agg}}} = 2a \int_0^{\infty} \frac{\exp(\beta V_{\text{tot}})}{(2a+h)^2 G(h)} dh \quad (7)$$

where  $V_{\text{tot}}$  is the total interparticle potential and  $k_{\text{s}}$  is the Smoluchowski diffusion-limited aggregation rate  $k_{\text{s}} = (8/3)k_{\text{B}}T/\mu$  with  $\mu$  the solvent viscosity. The hydrodynamics of two spheres approaching is given by  $G(h) = (6(h/a)^2 + 4(h/a))/(6(h/a)^2 + 13(h/a) + 2)$ . Combining eqs 6 and 7 and rewriting the colloidal concentration  $n_0$  in terms of the volume fraction  $\phi_0$  and the volume of one particle  $V_{\text{p}}$ , we can recover the expression

$$k_{\text{c}} = \frac{4\phi_0 k_{\text{B}}T}{3V_{\text{p}}W\mu} \quad (8)$$

This identity can be inserted into eq 5 to obtain an explicit form for the gelation time as a function of the sample material characteristics and interaction parameters

$$t_{\text{gel}} = \frac{3V_{\text{p}}W\mu}{8\phi_0 k_{\text{B}}T[(1+c)\phi_0/2]^{d_{\text{f}}/3}} \quad (9)$$

Gelation times of various samples, varying salt type in Figure 2, salt concentration, and Ludox concentration in Figure 3 were determined by checking when macroscopic samples no longer flowed. Clearly, there is a progressive shortening of gelation times switching samples with the same salt concentration, going from LiCl to NaCl, KCl, RbCl, and CsCl, and this is in agreement with the Hofmeister series. There are 4 orders of magnitude of difference in the gelation times (quite remarkable!) for the same concentrations of monovalent salts.

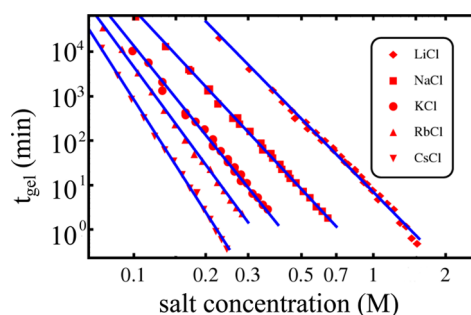


**Figure 2.** There is a very strong power law dependence (approximately  $-6$  exponent) between gelation time and salt concentration and a striking difference between the five monovalent salt species. The experimental observations (markers) are well recapitulated by the theoretical predictions (one parameter fits, as described in the text) (solid lines). Data are obtained from samples with volume fractions 0.13 and 0.14, and are undistinguishable. For each curve, the only free fit parameter is the hydration force amplitude  $F_0$ , which is a function dependent on the salt concentration. (See Figure 5.) The theory is calculated assuming volume fraction 0.133 and provides a match with the data for values of  $F_0$  well within the typical range of  $10^6$  to  $5 \times 10^8 \text{ Nm}^{-2}$  (ref 19).

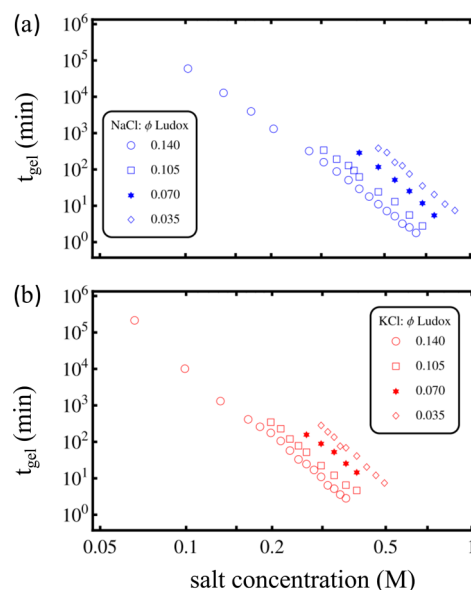


**Figure 3.** Power law dependence of gelation time with salt concentration and the strongly salt-specific gelation times (shown here are (a) NaCl and (b) KCl) are seen in samples with varying Ludox concentration. Values of the best fit power law exponents are listed in Table 1.

There is a clear power law dependence of the gelation times on the salt concentration, with exponents (see Table 1) all close to  $-6$ . There appears to be a decrease in power law exponent (to a more negative value) as the cation becomes more chaotropic. For samples with NaCl, the power law exponent decreases (becomes more negative) as the Ludox concentration decreases, but no clear trend is observed for samples with KCl. Reerink and Overbeek<sup>29</sup> found similar power law behavior for AgI colloids, with power law exponents from around  $-6$  to  $-11$ , depending on the particle size and surface potential. Other power law exponents had been reported in classical literature,<sup>29</sup> ranging from  $-2$  to  $-12$ . The value of  $-6$

**Table 1. Power Law Exponents for Gelation Times from the  $t_{\text{gel}}$  versus Salt Concentration Data in Figures 2 and 3<sup>a</sup>**

salt	volume fraction Ludox	exponent
KCl	0.140	$-6.27 \pm 0.24$
KCl	0.105	$-6.42 \pm 0.34$
KCl	0.070	$-5.92 \pm 1.06$
KCl	0.035	$-7.03 \pm 0.42$
NaCl	0.140	$-5.67 \pm 0.11$
NaCl	0.105	$-6.06 \pm 0.30$
NaCl	0.070	$-6.47 \pm 0.56$
NaCl	0.035	$-6.60 \pm 0.34$
LiCl	0.133	$-5.49 \pm 0.07$
NaCl	0.133	$-5.77 \pm 0.10$
KCl	0.133	$-6.68 \pm 0.15$
RbCl	0.133	$-7.33 \pm 0.06$
CsCl	0.133	$-8.44 \pm 0.10$

<sup>a</sup>Error quoted is the 95% confidence interval.

falls into this range and seems very robust in our silica colloid data.

A power law relation is also expected if the Ludox volume fraction is varied, at fixed salt concentration.<sup>25</sup> If the colloidal aggregation is taking place with fractal dimension  $d_f = 2.1$  (as is the case in the RLCA regime), then the exponent in this plot is expected to be  $-(d_f/3 + 1) = -1.7$ ; the data in Figure 4 show a

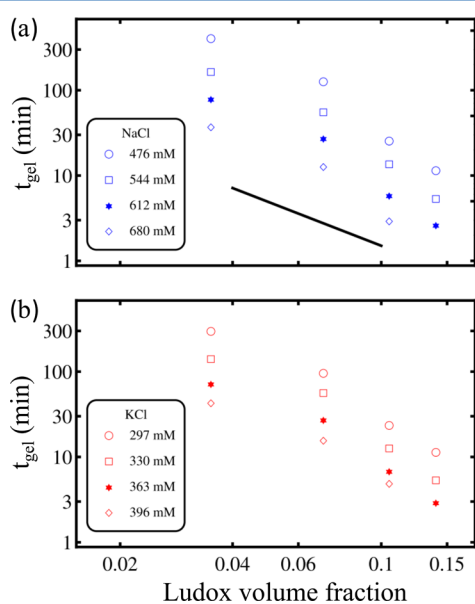


**Figure 4.** Gelation times also depend on the volume fraction  $\phi_{\text{Ludox}}$  of Ludox particles: (a) KCl and (b) NaCl. The solid line is a guide to the eye, illustrating the slope from a power law with exponent  $-1.7$ , which is expected for a fractal dimension of 2.1.

good agreement with this theoretical expectation. Note, however, that because (as explained later) we cannot assume to have a constant hydration force, we cannot use the data of Figure 4 to robustly go backward and extract the fractal dimension.

The theoretical framework previously outlined, along with the experimental data on the gelation times at varying salt concentration, now allows us to obtain the hydration parameters of the monovalent salts LiCl, NaCl, KCl, RbCl, and CsCl. The first question to address is how to define the

exponential decay length  $\lambda$  in eq 3. Throughout the literature this parameter has been varied within the range 0.2 to 1.0 nm<sup>19</sup> for different colloidal systems. It seems reasonable to us to set  $\lambda$  as the characteristic hydration diameter of the counterions ( $\text{Cs}^+ = 658$  pm,  $\text{Rb}^+ = 658$  pm,  $\text{K}^+ = 662$  pm,  $\text{Na}^+ = 716$  pm,  $\text{Li}^+ = 764$  pm).<sup>30</sup>

The second, more delicate question, is how to determine the two other unknown interaction parameters, which are the amplitude  $F_0$  of the hydration interaction (in eq 3) and the surface potential  $\psi_0$  (in eq 2).

Our first approach was to fix the hydration force constant  $F_0$  equal to a reasonable value from the literature,<sup>2</sup> and allow the surface potential to vary as a function of the salt concentration. Indeed, it might be expected that the association of counterions with silica surface groups will diminish the magnitude of the surface potential with increasing salt concentration, thus reducing the electrostatic repulsion and speeding up the gelation process.<sup>31</sup> This effect, while certainly present, is, however, far too small to justify by itself the rapid fall in the gelation times for increasing salt concentrations, as observed in Figures 2 and 3. Coupled to the fact that experimental  $\zeta$ -potential measurements have been observed to be relatively insensitive to counterion adsorption on the surface,<sup>32</sup> we proceeded to approximate the surface potential to be constant and set it equal to its dilute value of  $-30$  mV.<sup>33</sup> The second approach was therefore to proceed with the surface potential fixed, so that we could fit the experimental data in Figures 2 and 3, to obtain the hydration force constants  $F_0$  for each salt, and for each concentration. This is shown in Figures 5 and 6, as a

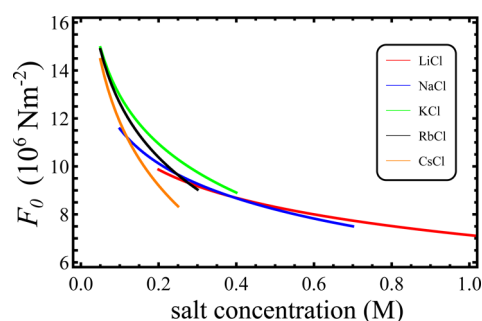


**Figure 5.** Hydration force constant  $F_0$  diminishes with increasing salt concentration. These values are obtained from samples with a volume fraction  $\phi_{\text{Ludox}}$  of 0.133.

function of salt concentration and particle volume fraction. It is clear from this framework that the reduction in  $F_0$ , and by extension in the repulsive hydration potential, upon increasing

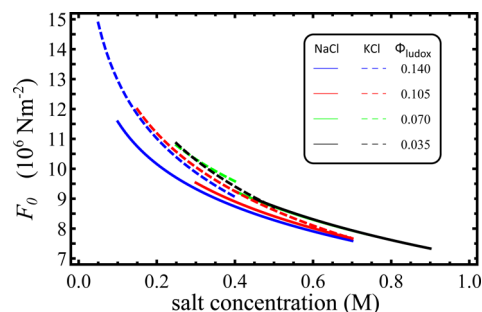


**Figure 6.** Hydration force constant  $F_0$  has a weak but systematic dependence on the particle volume fraction  $\phi_{\text{Ludox}}$ .

the salt concentration, is what controls the power-law relationship observed in Figures 2 and 3.

The hydration force magnitude values  $F_0$ , are obtained at each salt concentration ( $c$ ) from a one-parameter fit to the experimental data points in Figure 3. The resulting functions  $F_0(\phi(c))$  are shown in Figure 5 (five salts) and Figure 6 (four different values of the particle volume fraction  $\phi_{\text{Ludox}}$ ). Three trends are visible: (1)  $F_0(c)$  is higher for KCl than for any of the other ions; this means a nonmonotonic behavior in terms of ionic size. (2)  $F_0(c)$  increases as Ludox concentration decreases. (3)  $F_0(c)$  decreases as salt concentration increases. If our effective potential is valid, we have to assume all three effects are related to the association of the counterions with silica surface charge groups (or else other factors might be contributing to the interaction and are being assimilated into these  $F_0$  trends).

A plausible expected behavior is that it is more difficult for the smaller, more hydrated monovalent cations to approach and thus associate with the surface hydroxyl groups. Counterions adsorbed on the silica surface act as a repulsive force between particles. This explains why the hydration potential  $V_h$  increases monotonically as a function of the hydration diameter. (See Figure 7.) Note that because  $V_h \propto F_0 \lambda^2$  eq 3),

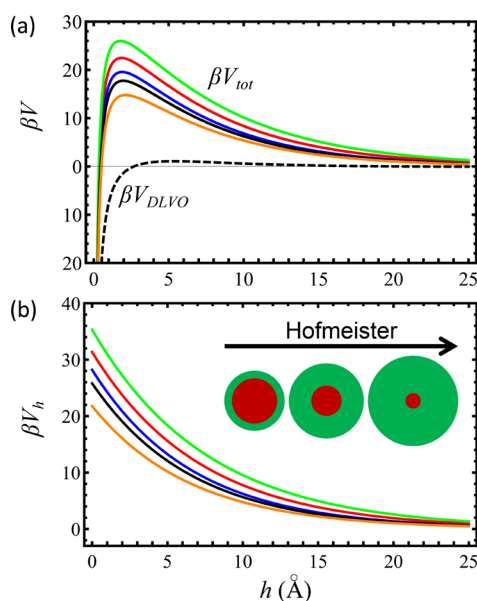


**Figure 7.** Salt-specific repulsion is very important at short-range, as shown in (a) by comparing the total interparticle potential ( $V_{\text{tot}}$ , solid line) to the potential ( $V_{\text{DLVO}}$ , dashed line) without the hydration potential  $V_h$  and in (b) by plotting the hydration contribution by itself. The potentials decrease with salt species in the order LiCl-NaCl-KCl-RbCl-CsCl. Salt concentration is equal to 0.3 M for both plots.

the trend of  $F_0$  (Figures 5 and 6, which is observation (1) above, is more complex. A greater particle volume fraction corresponds to a greater total surface area, which is consistent with diminishing counterion association per unit surface area and slight reduction of  $F_0$ , which is observation (2) above. Also consistent with this picture is the fact that as we increase the salt concentration the proportion of surface charge groups remaining free for counterion association dwindles and the ion-specific values of  $F_0$  begin to converge. Figure 7 shows that the hydration potential increases as the hydration diameter  $\lambda$  lengthens, with the ordering of the salts by the relative strength

of repulsive hydration forces remaining the same over all distances. Therefore, the greater the hydration diameter of the counterion the more long-ranged the hydration force becomes and the greater the potential barrier to gelation. As a key result, the gelation time increases together with the hydration diameter of the ions in the Hofmeister series.

In Figure 8, the hydration potential is observed to be a short-ranged monotonically decreasing function of the salt

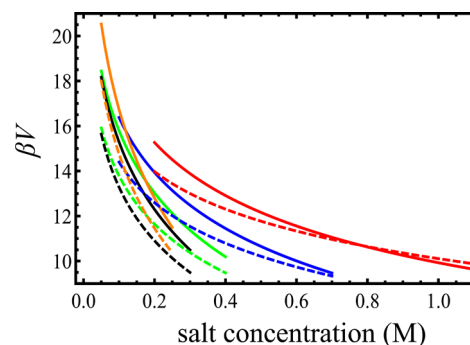


**Figure 8.** With increasing salt concentration, the hydration potential decreases. The interparticle separation is set here at the hydration diameter for each salt species. Solid lines are  $\beta V_{\text{tot}}$  and dashed lines are  $\beta V_h$ ; same color scheme as in 7.

concentration (observation (3) previously considered). The precise origin of this effect is not obvious. In our simple picture of counterion adsorption, we expect more ions to adsorb the higher the bulk concentration. A possibility, similarly to what is proposed in ref 5, is that one needs to consider a loss of hydration shell when many ions adsorb, with a corresponding decline in repulsion. A final point we should remind the reader is that the surface charge density in the DLVO terms has been kept constant; this is unlikely to be strictly correct, but it is very difficult to do otherwise with the data at hand.<sup>31</sup> Also, there are no experimental techniques to accurately evaluate the surface potential, and standard zeta-potential measurements are not adequate for this task. So the question of whether this particular trend originates from some physical force or change in conditions at the gap or an external force such as the bulk osmotic pressure remains to be properly addressed in future studies.

Of particular interest to this work, Trompette and coworkers have described in a series of papers<sup>33–35</sup> the effect of  $\text{NH}_4^+$  and  $\text{Na}^+$  on the stability of colloidal silica and found that samples with  $\text{NH}_4^+$  aggregated much faster than those with  $\text{Na}^+$ . They ascribed this to the different degrees of hydration of the ions. For the experiments described in this paper, only LiCl, NaCl, KCl, RbCl, and CsCl were studied because the ammonium salt ion is somewhat acidic, and the pH itself also affects stability of colloidal silica.

Experimental papers investigating short-ranged hydration forces have classically employed surface force apparatus (SFA) and more recently also atomic force microscopy (AFM). These techniques can be applied to measure the forces between smooth solid surfaces, lipid bilayers, and biomembrane surfaces.<sup>22</sup> Some of the most recent studies include the use of AFM to estimate short-ranged hydration forces induced by multivalent salts,<sup>36,37</sup> the investigation of ion-specific Hofmeister effects between planar single-crystal sapphire,<sup>38</sup> and the measurement of charge inversion as a function of pH and salt concentration. These studies are in agreement<sup>39,40</sup> with the

trends presented here, while under other conditions the Hofmeister series is in reverse order,<sup>41</sup> but we have not found experiments that can be directly compared with our results. We also note that our modeling shows that variations in the surface potential are insignificant compared with the dominant short-ranged hydration forces at close surface-to-surface separations. Ion-specific double-layer pressure has been calculated using the full nonlinear Poisson–Boltzmann equation with the addition of the ionic dispersion energy between the ions and the two interfaces.<sup>42</sup> By treating the electrodynamic ionic dispersion potentials on the same nonlinear level as electrostatic potential, the ion-specific Hofmeister effects are recovered. We believe that there is great scope to combine studies such as this with experimental approaches such as in this manuscript to help isolate and calibrate the various possible mechanisms underpinning the hydration forces and bridge the gap between molecular and macroscopic observation.

In conclusion, systematic experiments were carried out quantifying the gelation kinetics as a function of monovalent salt species. By using a simple model for the kinetics of cluster aggregation to fit experimental data of gelation times, under different salt conditions, for the first time it was possible to extract the magnitude of a non-DVLO hydration repulsion, that has a range set by the solvated diameter of the counterion. The very simple non-DVLO term used here is obviously coarse graining the detailed molecular mechanisms (the ordered “rigid” water layers repelling each other and the energy required to “squeeze” these away as the particles approach contact) and is an effective semiempirical term. This approach is powerful because experiments can then be readily fitted by a single parameter, the amplitude of repulsion force ( $F_0$ , function of salt concentration). The latter decreases with increasing salt concentration due to desolvation of the counterions upon adsorption on the surface. The key finding is that the hydration repulsion correlates positively with the chaotropic nature and the size of the cation species. This framework and the molecular-level mechanism proposed here can be used in the future to devise tunable gelation protocols of nanoparticles by choosing the salt type.

## METHODS

All samples studied consist of colloidal silica, water, and salt in different concentrations. Commercial silica colloids of Ludox HS-30 (Sigma-Aldrich) were used. Ludox HS size measurements vary from 16.7<sup>43</sup> to 18.5 nm<sup>44</sup> diameter, and we have taken 17 nm diameter as a value in our calculations.

The Ludox was filtered prior to use, using Millipore Millex GS 0.22  $\mu\text{m}$  filters, to ensure the removal of larger aggregates. The resulting Ludox “stock” used in most of the experiments had a density of 1.23 g/mL and contained 31.5% silica by weight. The pH of the original Ludox suspension (before filtration and dilution) was 9.8 (determined by the manufacturer) and was not regulated during the experiments. Stock solutions of salt were prepared using LiCl (99.0%, Sigma-Aldrich and 99%, Acros), NaCl (99.0%, Sigma-Aldrich and analysis grade, Merck), KCl (99.9%, Fischer and 99+%, Acros), RbCl (99.8+%, Acros), and CsCl (99+%, Acros). All water used for preparation of stock solutions and samples was of Millipore grade.

The salt solution was always added last to make the final sample of 1 mL volume. All samples were mixed on a vortex mixer for  $\sim 10$  s immediately after the addition of salt stock.

The gelation time was determined on a macroscopic scale, by gently inverting the vials to observe the presence (or not) of flow. When there was no discernible flow for  $\sim 1$  s, the sample was judged to be gelled. This criterion is somewhat arbitrary but was strictly adhered to, so that results of different samples are consistent. Figure 1c shows photographs of a sample before and after its gelation time.

Preliminary runs were carried out, so that the gelation time was approximately known. This ensured that subsequent samples were not inverted unnecessarily. (We did not notice in any case correlations between the gelation time and the frequency of inspection.) Identical samples prepared on different days did sometimes show different gelation times, which could be due to small temperature changes or minor differences in sample composition or preparation. These differences were never very large ( $\sim 10\%$ ) and do not affect the observed trends.

## ASSOCIATED CONTENT

### Supporting Information

Details of the complete expressions for the attractive van der Waals potential and electrostatic interaction terms used in this work. The Supporting Information is available free of charge on the ACS Publications website at DOI: 10.1021/acs.jpcllett.5b01300.

## AUTHOR INFORMATION

### Corresponding Authors

\*E-mail: az302@cam.ac.uk.

\*E-mail: pc245@cam.ac.uk.

### Author Contributions

<sup>||</sup>M.v.d.L. and B.O.C. are joint first authors.

### Notes

The authors declare no competing financial interest.

## ACKNOWLEDGMENTS

We acknowledge useful discussions with A. Routh and L. Cipelletti, preliminary work by H. Hong, and financial support from Unilever Plc (E.S.); the Ernest Oppenheimer Fellowship at Cambridge (to first June 2014), and by the Technische Universität München Institute for Advanced Study, funded by the German Excellence Initiative and the European Union Seventh Framework Programme under grant agreement 291763 (A.Z.); the Winton Programme for the Physics of Sustainability (B.O.C.). All data needed to support and reproduce these results are presented within the paper.

## REFERENCES

- (1) Hunter, R. J. *Foundations of Colloid Science*; Oxford University Press: Oxford, U.K., 1986; Vol. 1.
- (2) Israelachvili, J. N. *Intermolecular and Surface Forces*; Academic Press: San Diego, CA, 2011.
- (3) Everett, D. H. *Basic Principles of Colloid Science*; Royal Society of Chemistry: London, U.K., 1988.
- (4) Bostrom, M.; Williams, D. R. M.; Ninham, B. W. Specific Ion Effects: Why DLVO Theory Fails for Biology and Colloid Systems. *Phys. Rev. Lett.* **2001**, *87*, 168103.
- (5) Parsons, D. F.; Bostrom, M.; Nostro, P. L.; Ninham, B. W. Hofmeister Effects: Interplay of Hydration, Nonelectrostatic Potentials, and Ion Size. *Phys. Chem. Chem. Phys.* **2011**, *13*, 12352–12367.
- (6) Salis, A.; Ninham, B. W. Models and Mechanisms of Hofmeister Effects in Electrolyte Solutions, and Colloid and Protein Systems Revisited. *Chem. Soc. Rev.* **2014**, *43*, 7358–7377.

- (7) Ninham, B. W.; Yaminsky, V. Ion Binding and Ion Specificity: The Hofmeister Effect and Onsager and Lifshitz Theories. *Langmuir* **1997**, *13*, 2097–2108.
- (8) Kunz, W.; Henle, J.; Ninham, B. W. Zur Lehre von der Wirkung der Salze (about the science of the effect of salts): Franz Hofmeister's historical papers. *Curr. Opin. Colloid Interface Sci.* **2004**, *9*, 19–37.
- (9) Piazza, R.; Pierno, M. Protein Interactions near Crystallization: A Microscopic Approach to the Hofmeister Series. *J. Phys.: Condens. Matter* **2000**, *12*, 443–449.
- (10) Huang, H.; Ruckenstein, E. Effect of Hydration of Ions on Double-Layer Repulsion and the Hofmeister Series. *J. Phys. Chem. Lett.* **2013**, *4*, 3725–3727.
- (11) dos Santos, A. P.; Levin, Y. Ion Specificity and the Theory of Stability of Colloidal Suspensions. *Phys. Rev. Lett.* **2011**, *106*, 167801.
- (12) Paunov, V. N.; Dimova, R. I.; Kralchevsky, P. A.; Broze, G.; Mehreteab, A. The Hydration Repulsion between Charged Surfaces as an Interplay of Volume Exclusion and Dielectric Saturation Effects. *J. Colloid Interface Sci.* **1996**, *182*, 239–248.
- (13) Lyklema, J. Simple Hofmeister Series. *Chem. Phys. Lett.* **2009**, *467*, 217–222.
- (14) Paunov, V. N.; Binks, B. P. Analytical Expression for the Electrostatic Disjoining Pressure taking into account the Excluded Volume of the Hydrated Ions between Charged Interfaces in Electrolyte. *Langmuir* **1999**, *15*, 2015–2021.
- (15) Kralchevsky, P. A.; Danov, K. D.; Basheva, E. S. Hydration Force due to the Reduced Screening of the Electrostatic Repulsion in Few-Nanometer-Thick Films. *Curr. Opin. Colloid Interface Sci.* **2011**, *16*, 517–524.
- (16) Parsons, D. F.; Ninham, B. W. Charge Reversal of Surfaces in Divalent Electrolytes: The Role of Ionic Dispersion Interactions. *Langmuir* **2010**, *26*, 6430–6436.
- (17) Boroudjerdi, H.; Kim, Y. W.; Naji, A.; Netz, R. R.; Schlagberger, X.; Serr, A. Statics and Dynamics of Strongly Charged Soft Matter. *Phys. Rep.* **2005**, *416*, 129–199.
- (18) Liu, X.; Li, H.; Li, R.; Xie, D.; Ni, J.; Wu, L. Strong Non-Classical Induction Forces in Ion-Surface Interactions: General Origin of Hofmeister Effects. *Sci. Rep.* **2014**, *4*, 5047.
- (19) Jia, Z.; Gauer, C.; Wu, H.; Morbidelli, M.; Chittofrati, A.; Apostolo, M. A Generalized Model for the Stability of Polymer Colloids. *J. Colloid Interface Sci.* **2006**, *302*, 187–202.
- (20) Vanni, M.; Baldi, G. Coagulation Efficiency of Colloidal Particles in Shear Flow. *Adv. Colloid Interface Sci.* **2002**, *97*, 151–177.
- (21) Sader, J.; Carnie, S. L.; Chan, D. Y. C. Accurate Analytic Formulas for the Double Layer Interaction between Spheres. *J. Colloid Interface Sci.* **1995**, *171*, 46–54.
- (22) Israelachvili, J.; Wennerstrom, H. Role of Hydration and Water Structure in Biological and Colloidal Interactions. *Nature* **1996**, *379*, 219–225.
- (23) Marcelja, S.; Radic, N. Repulsion of Interfaces due to Boundary Water. *Chem. Phys. Lett.* **1976**, *42*, 129–130.
- (24) Zacccone, A.; Wu, H.; Lattuada, M.; Morbidelli, M. Charged Molecular Films on Brownian Particles: Structure, Interactions, and Relation to Stability. *J. Phys. Chem. B* **2008**, *112*, 6793–6802.
- (25) Zacccone, A.; Crassous, J. J.; Ballauff, M. Colloidal Gelation with Variable Attraction Energy. *J. Chem. Phys.* **2013**, *138*, 104908.
- (26) Lin, M. Y.; Lindsay, H. M.; Weitz, D. A.; Ball, R. C.; Klein, R.; Meakin, P. Universal Reaction-Limited Colloid Aggregation. *Phys. Rev. A: At., Mol., Opt. Phys.* **1990**, *41*, 2005–2020.
- (27) Lin, M. Y.; Lindsay, H. M.; Weitz, D. A.; Ball, R. C.; Klein, R.; Meakin, P. Über die Stabilität und Aufladung der Aerosole. *Z. Phys.* **1934**, *89*, 736–743.
- (28) Mewis, J.; Wagner, N. J. *Colloidal Suspension Rheology*; Cambridge University Press: Cambridge, U.K., 2012.
- (29) Reerink, H.; Overbeek, J. Th. G. The Rate of Coagulation as a Measure of the Stability of Silver Iodide Sols. *Discuss. Faraday Soc.* **1954**, *18*, 74–84.
- (30) Conway, B. E. *Ionic Hydration in Chemistry and Biophysics*; Elsevier: Amsterdam, The Netherlands, 1981.
- (31) Ninham, B. W.; Parsegian, V. A. Electrostatic Potential between Surfaces bearing Ionizable Groups in Ionic Equilibrium with Physiologic Saline Solution. *J. Theor. Biol.* **1971**, *31*, 405–428, DOI: 10.1016/0022-5193(71)90019-1.
- (32) Merk, V.; Rehbock, C.; Becker, F.; Hagemann, U.; Nienhaus, H.; Barcikowski, S. In Situ Non-DLVO Stabilization of Surfactant-Free, Plasmonic Gold Nanoparticles: Effect of Hofmeister's Anions. *Langmuir* **2014**, *30*, 4213–4222.
- (33) Trompette, J. L.; Meireles, M. Ion-Specific Effect on the Gelation Kinetics of Concentrated Colloidal Silica Suspensions. *J. Colloid Interface Sci.* **2003**, *263*, 522–527.
- (34) Trompette, J. L.; Clifton, M. J. Influence of Ionic Specificity on the Microstructure and the Strength of Gelled Colloidal Silica Suspensions. *J. Colloid Interface Sci.* **2004**, *276*, 475–482.
- (35) Trompette, J. L.; Clifton, M. J.; Bacchin, P. Ion-Specific Repulsive Interactions in Colloidal Silica Dispersions evidenced through Osmotic Compression Measurements and Implication in Frontal Ultrafiltration Experiments. *J. Colloid Interface Sci.* **2005**, *290*, 455–461.
- (36) Montes Ruiz-Cabello, F. J.; Trefalt, G.; Maroni, P.; Borkovec, M. Accurate Predictions of Forces in the Presence of Multivalent Ions by Poisson-Boltzmann Theory. *Langmuir* **2014**, *30*, 4551–4555.
- (37) Montes Ruiz-Cabello, F. J.; Moazzami-Gudarzi, M.; Elzbiaciak-Wodka, M.; Maroni, P.; Labbez, C.; Borkovec, M.; Trefalt, G. Long-Ranged and Soft Interactions between Charged Colloidal Particles induced by Multivalent Ions. *Soft Matter* **2015**, *11*, 1562–1571.
- (38) Lützenkirchen, J. Specific Ion Effects at Two Single-Crystal Planes of Sapphire. *Langmuir* **2013**, *29*, 7726–7734.
- (39) Franks, G. V. Zeta Potentials and Yield Stresses of Silica Suspensions in Concentrated Monovalent Electrolytes: Isoelectric Point Shift and Additional Attraction. *J. Colloid Interface Sci.* **2002**, *249*, 44–51.
- (40) Jiménez, M. L.; Delgado, A. V.; Lyklema, J. Hydrolysis versus Ion Correlation Models in Electrokinetic Charge Inversion: Establishing Application Ranges. *Langmuir* **2012**, *28*, 6786–6793.
- (41) Morag, J.; Dishon, M.; Sivan, U. The Governing Role of Surface Hydration in Ion Specific Adsorption to Silica: An AFM-based Account of the Hofmeister Universality and its Reversal. *Langmuir* **2013**, *29*, 6317–6322.
- (42) Boström, M.; Deniz, V.; Franks, G.; Ninham, B. W. Extended DLVO theory: Electrostatic and Non-Electrostatic Forces in Oxide Suspensions. *Adv. Colloid Interface Sci.* **2006**, *123*, 5–15.
- (43) Chen, G.; Yu, W.; Singh, D.; Cookson, D.; Routbort, J. Application of SAXS to the Study of Particle-Size-Dependent Thermal Conductivity in Silica Nanofluids. *J. Nanopart. Res.* **2008**, *10*, 1109–1114.
- (44) Van der Meeren, P.; Saveyn, H.; Bogale Kassa, S.; Doyen, W.; Leysen, R. Colloid-Membrane Interaction Effects on Flux Decline during Cross-Flow Ultrafiltration of Colloidal Silica on Semi-Ceramic Membranes. *Phys. Chem. Chem. Phys.* **2004**, *6*, 1408–1412.